

## **Investigating Mould Heat Transfer in Thin Slab Casting with CON1D**

Begoña Santillana  
Corus RD&T SCC/CMF  
P.O. Box 10000  
1970 CA IJmuiden, The Netherlands  
Tel.: +31(0) 251 493066  
Fax: +31(0) 251 470236  
E-mail: begona.santillana@corusgroup.com

Brian G. Thomas  
University of Illinois at Urbana-Champaign  
1206 West Green Street  
Urbana, IL 61801  
Tel.: (217) 333-6919  
Fax: (217) 244-6534  
E-mail: bgthomas@uiuc.edu

Arie Hamoen  
Corus RD&T SCC  
E-mail: arie.hamoen@corusgroup.com

Lance C. Hibbeler  
University of Illinois at Urbana-Champaign  
E-mail: lhibbel2@uiuc.edu

Arnoud Kamperman  
Corus Strip Products IJmuiden/ Direct Sheet Plant  
P.O. Box 10000  
1970 CA IJmuiden, The Netherlands  
E-mail: arnoud.kamperman@corusgroup.com

Willem van der Knoop  
Corus RD&T SCC/CMF  
E-mail: willem.van-der-knoop@corusgroup.com

Key words: thin-slab casting, numerical modelling, funnel mould, continuous casting of steel

### **INTRODUCTION**

Mould heat transfer in continuous casting is important to mould life, surface quality, breakouts and many aspects of the process. Heat transfer in the thin slab casting mould is being investigated with the 1-D heat transfer model, CON1D. To account for the multidimensional thermal behaviour around the cooling channels of the funnel mould, a three-dimensional finite-element model, developed using ABAQUS, is applied to find correction factors that enable CON1D to predict accurately temperature at thermocouple locations. The model calculations have been validated using an extensive database of plant process parameters obtained from the Corus Direct Sheet Plant in IJmuiden, including measurements of mould powder consumption, oscillation mark shape, mould temperature, and heat removal. The improved CON1D model is applied here to predict casting behaviour for different speeds and to investigate the effect of mould plate thickness. The results will be used to extrapolate standard practices to higher casting speeds and new mould designs.

## CON1D MODEL DESCRIPTION

The heat transfer model, CON1D<sup>1</sup>, models several aspects of the continuous casting process, including shell and mould temperatures, heat flux, interfacial microstructure and velocity, shrinkage estimates to predict taper, mould water temperature rise and convective heat transfer coefficient, interfacial friction and many other phenomena. The heat transfer calculations are one-dimensional through the thickness of the shell and interfacial gap with two-dimensional conduction calculations in the mould. An entire simulation requires only a few seconds on a modern PC.

Heat transfer in the mould is computed assuming a slab with attached rectangular blocks that form the cooling-water channels and act as heat transfer fins. The process parameters used in this analysis are typical values used with the Corus Direct Sheet Plant (DSP) thin-slab continuous casting machine in IJmuiden, Netherlands. Key parameters include casting speeds of 4.5 and 5.2 m/min, pour temperature of 1545 °C, meniscus level of 100 mm below the top of the funnel mould, casting a 0.045 %C steel. To model accurately the complex geometry of the funnel mould and water slots, an offset methodology<sup>2</sup> is applied to calibrate the model to match the predictions of a full three-dimensional finite element model using ABAQUS<sup>3</sup>.

### Narrow face

To create the simple mould geometry for CON1D, the actual narrow face cross-section (black) was transformed into the one-dimensional rectangular channel geometry (red), as shown in Figure 1. The bolt holes are 22 mm in diameter and 20.5 mm deep; the thermocouple holes are 4 mm in diameter and extend into the mould such that they are 20 mm from the hot face.

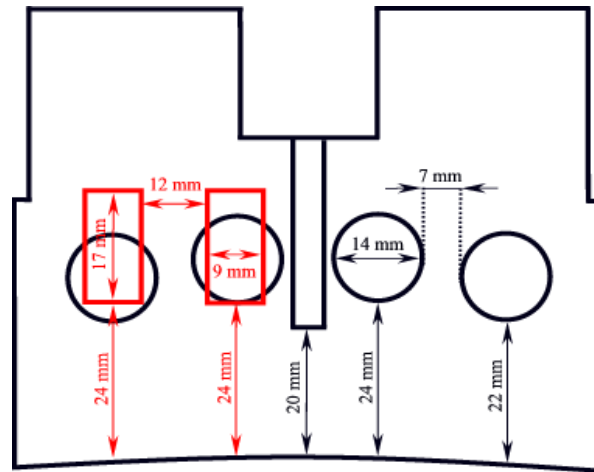
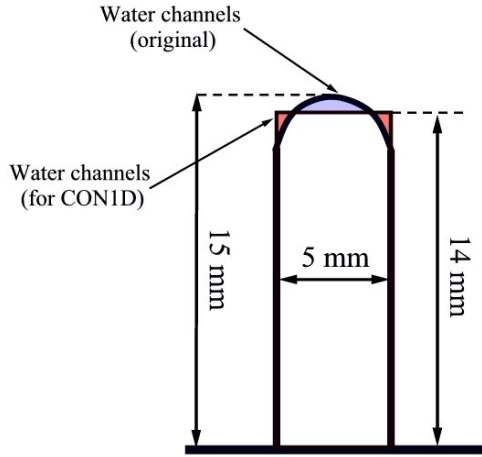


Figure 1. Narrow face mould geometry and CON1D simplification (overlaid on left side in red)

To approximate the actual geometry, the shortest distance between the water channels and the hot face was maintained at 24 mm and the pitch between the channels similarly was set to 12 mm. To match the water flow rate, the dimensions of the rectangular channels were chosen to keep the cross-sectional area about the same as that of the actual 14 mm diameter channels. In addition, to maintain heat transfer characteristics, the channel width was chosen to be about two-thirds of the diameter of the actual round channel. These two considerations yield a 9 mm by 17 mm channel and a 41 mm thick mould. CON1D aims only to model a typical section through the mould and cannot predict variations in the direction around the mould perimeter, such as corner effects.

### Wide Face

Water channels in the wide face required similar dimensional adjustments for CON1D. The actual water channels are spaced 5 mm apart and are 5 mm wide and 15 mm deep, but with rounded roots. As shown in Figure 2, the CON1D water channels are 5 mm wide but 14 mm deep, so that outer (red) areas compensate for the upper (blue) area and roughly match the real cross sectional area. The mould thickness was maintained at 35 mm. As shown in Figure 3, this keeps the channels at a constant distance of 21 mm from the hot face, in comparison with the real mould, where closest point of the rounded channel root is 20 mm from the hot face. The bolt holes have the same dimensions as on the narrow face, but on the wide face the thermocouple holes extend into the mould such that they are 15 mm from the hot face.



**Figure 2. Wide face water slot & CON1D simplification**

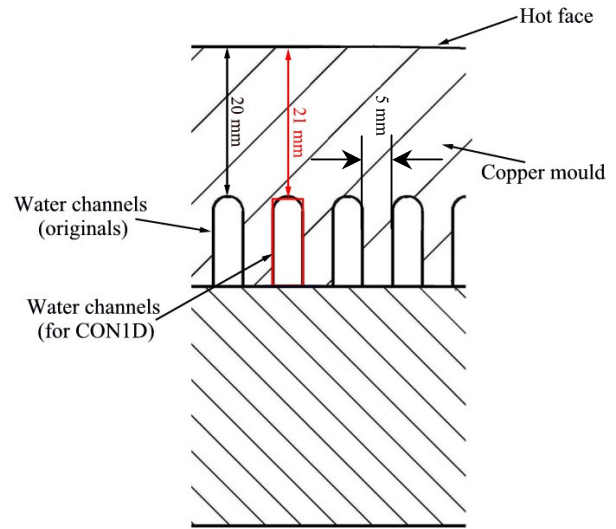


**Figure 3. Wide face mould geometry**

### CON1D MODEL OFFSET DETERMINATION

To enable CON1D to predict accurately the temperatures of thermocouples, it must be calibrated using a three-dimensional heat transfer calculation, to determine an offset distance for each mould face to adjust the modelled depth of the thermocouples.

#### Narrow Face

Two different three-dimensional heat transfer models were developed of the mould copper narrow faces (end plates) using ABAQUS 6.6-1. The first was a small, symmetric section of the mould geometry containing one quarter of a single thermocouple, which was used to determine the offset for CON1D. The second was a complete model of one symmetric half of the entire mould plate, used to determine an accurate temperature distribution including the effects of all geometric features and to evaluate the CON1D model.

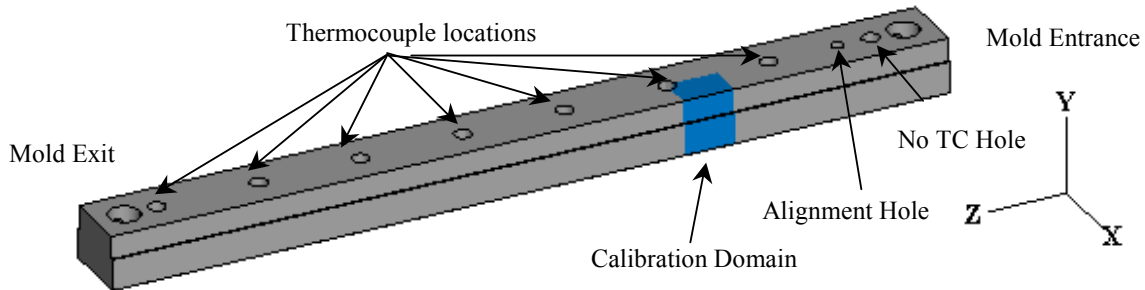


**Figure 4. Location of calibration domain**

To compare properly the finite-element model with CON1D, identical conditions were applied to both models. Figure 4 highlights the location of this “calibration section” in the entire mould piece, and Figure 5 shows the geometry and simplified boundary conditions. The applied heat flux  $Q$  to the hot face is constant and uniform, as are the thermal conductivity  $k$  of the mould, the convective heat transfer coefficient  $h$  and the water temperature  $T_\infty$  applied to the water channel surfaces. Unlabelled (grey) surfaces are insulated.

The finite-element mesh used 45840 mixed (hexahedrons, tetrahedrons and wedges) quadratic elements and ran in 80 seconds (wall clock) on a 2.0 GHz Intel Core2 Duo PC. Figure 6 shows the resulting temperature contour plot and identifies the location of the thermocouple temperature, as well as the face from which further data were extracted. The maximum temperature of 296 °C is found on the hot face corner, which is 20.5 °C hotter than the hot face centerline.

The temperature profiles along four paths are shown in Figure 7, in which a linear temperature gradient is evident between the hot face and the water channels. The temperature variation between these paths is small, with only 2 °C difference across the hot face in the vicinity of the paths. The lowest temperature is found on the back (cold face side) of the water channel (Path 3). The missing copper around the thermocouple causes the local temperature to rise about 10 °C, however. To account for this effect in CON1D, an offset distance is applied to the simulated depth of the thermocouples.

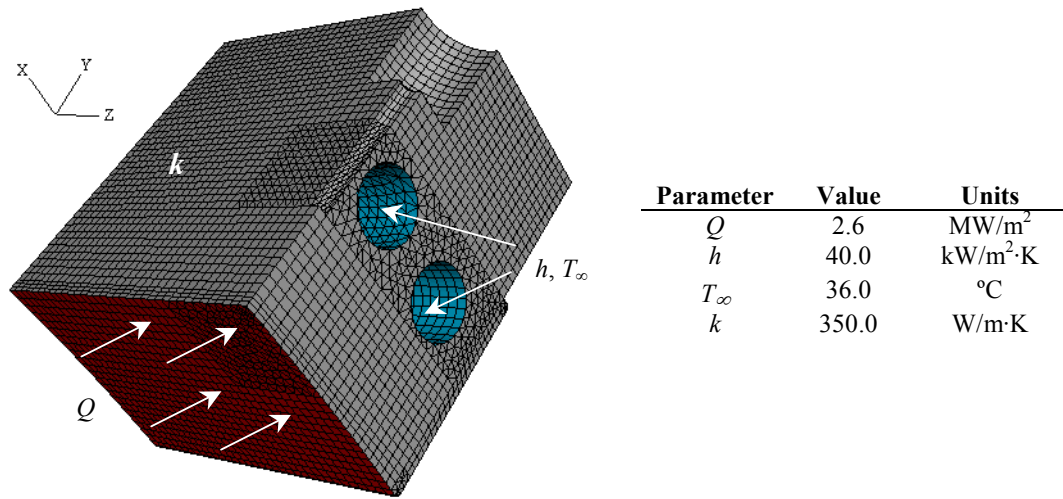


Figure 5. Narrow face boundary conditions and properties

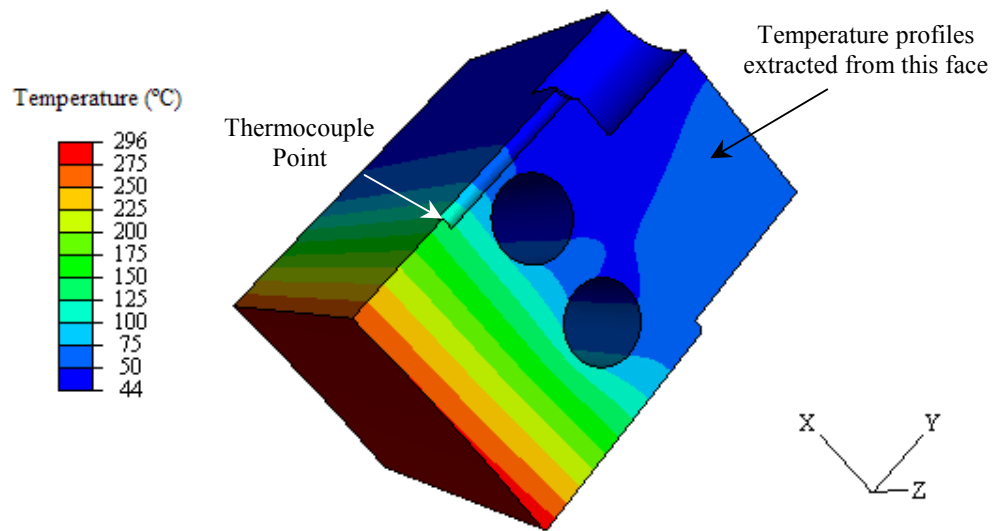


Figure 6. Narrow face calibration results

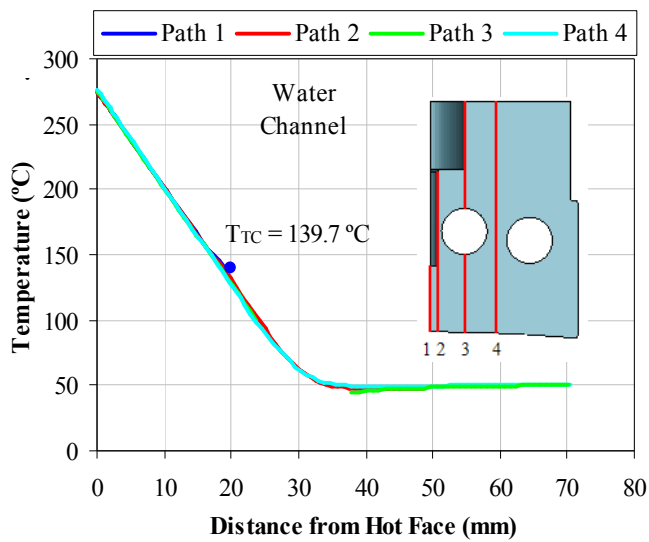


Figure 7. Temperature profiles in narrow face

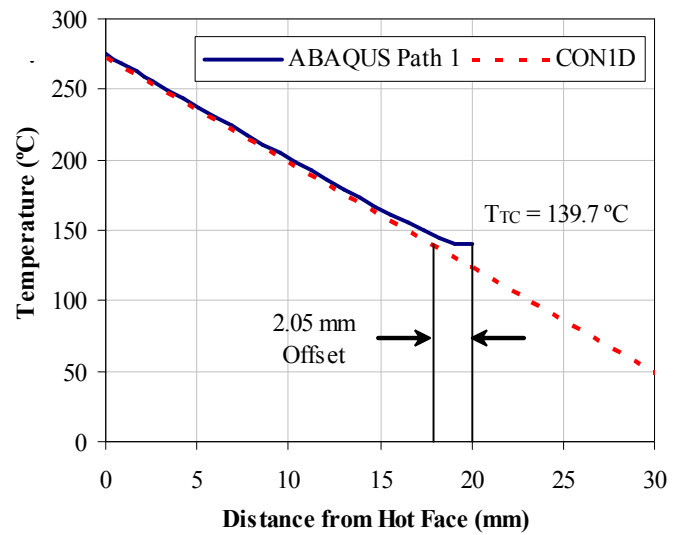


Figure 8. Determination of offset

An offset distance enables the one-dimensional model to relate accurately thermocouple temperatures by accounting for 3D conduction effects from the complex local geometry<sup>2</sup>. The difference in position between the thermocouples in the mould and in the model is called an “offset” and is the distance the thermocouple position is shifted when input to the CON1D model.

Figure 8 compares the temperature distribution of CON1D with the Path 1 results from Figure 7. Although CON1D cannot capture the localized effects of the complex geometric features, the 3-D thermocouple temperature can be found by “moving” the thermocouple to a new location closer to the hot face. This small “offset distance,” allows accurate thermocouple temperatures to be predicted by CON1D. This offset of the thermocouple depth can be determined from Equation (1) using the CON1D temperature profile as follows:

$$d_{offset} = (T_{TC} - T_{hf}) \frac{dx}{dT} - d_{TC} = (139.7 - 273.16)^\circ\text{C} \cdot \frac{30 \text{ mm}}{(50.21 - 273.16)^\circ\text{C}} - 20 \text{ mm} = 2.05 \text{ mm} \quad (1)$$

Where  $d_{offset}$  is the offset distance (mm)  
 $T_{TC}$  is thermocouple temperature from ABAQUS ( $^\circ\text{C}$ )  
 $T_{hf}$  is the thermocouple temperature from CON1D ( $^\circ\text{C}$ )  
 $dx/dT$  is the inverse of the temperature gradient from CON1D (mm/ $^\circ\text{C}$ )  
 $d_{TC}$  is the actual depth of the thermocouple from the hot face (mm)

Figure 8 also shows that CON1D is able to match the 3D results for about 12mm into the mould, or two-thirds of the distance from the hot face to the thermocouple.

### Wide Face

Following the same procedure used in the narrow face, the offset distance for the wide face was also calculated. The boundary conditions and properties were maintained the same as in the narrow face. A top view of these conditions and the 3-D temperature distribution is plotted in Figure 9.

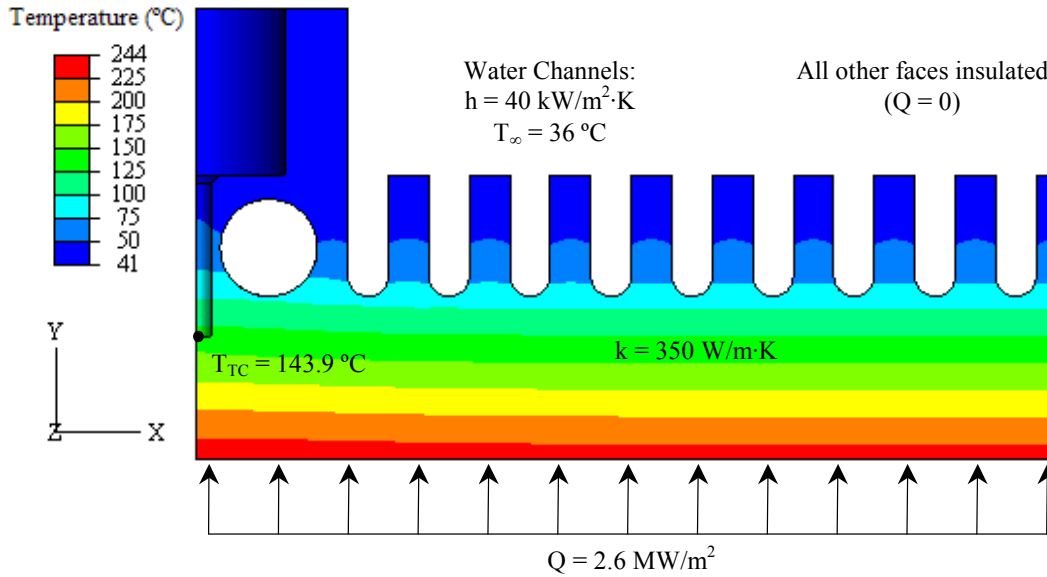


**Figure 9. Wide face calibration domain with input parameters**

The thermocouples in the real wide face are positioned 15 mm from the hot face and the offset was found to be 2.41 mm, meaning that the thermocouples in CON1D should be 2.41 mm closer to the hot face to produce accurate thermocouple predictions.

### 3D MOLD TEMPERATURES AND CON1D MODEL VERIFICATION

Having calibrated the CON1D model by determining the offset distance, both the full three-dimensional model and CON1D simulation were run using realistic boundary conditions for the mould.

#### Narrow Face

One symmetric half of the entire three-dimensional narrow face geometry was analysed in ABAQUS, using the DFLUX and FILM user subroutines to vary realistically heat flux and water temperature down the mould as given in Figure 10. Other parameters were maintained as in Figure 5. This ABAQUS model used 468583 quadratic tetrahedron elements and required 7.1 minutes (wall clock) to analyse.

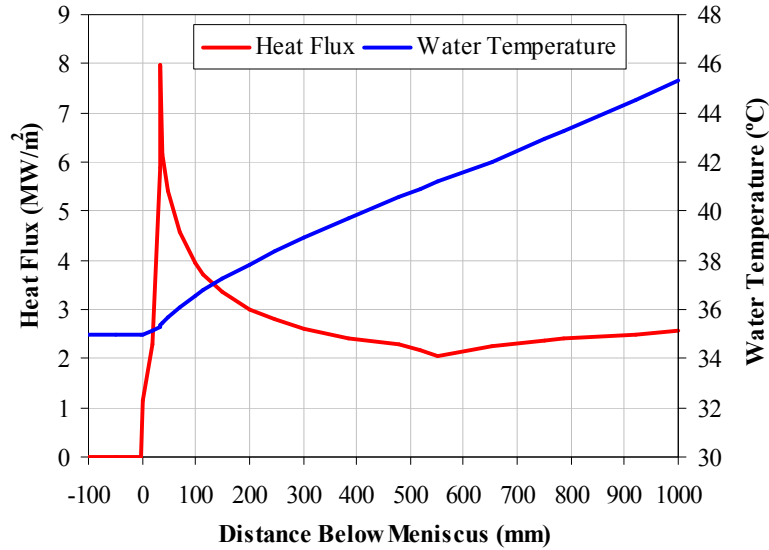


Figure 10. CON1D output heat flux and water temperature profiles as input to ABAQUS

Figure 11 shows the temperature contours from the three-dimensional model of the entire mould narrow face. Localized three-dimensional effects are observed near the peak heat flux region and at mould bottom. The cooler spot around the center of the hot face corresponds to an inflection point in the heat flux curve. The highest temperatures occur at the small-filleted corners of the mould at the peak heat flux, because they are furthest away from the water channels.

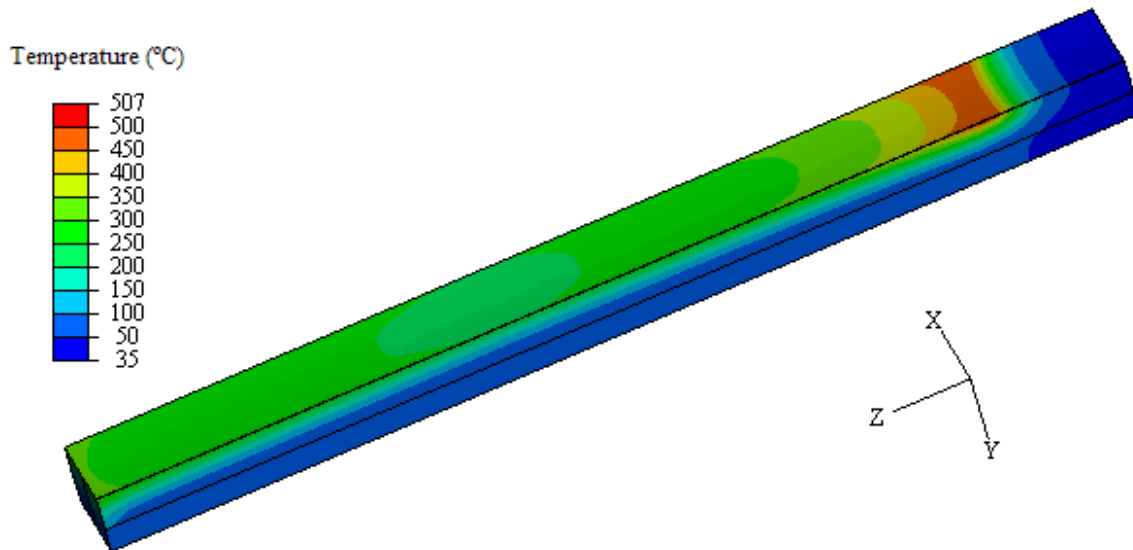
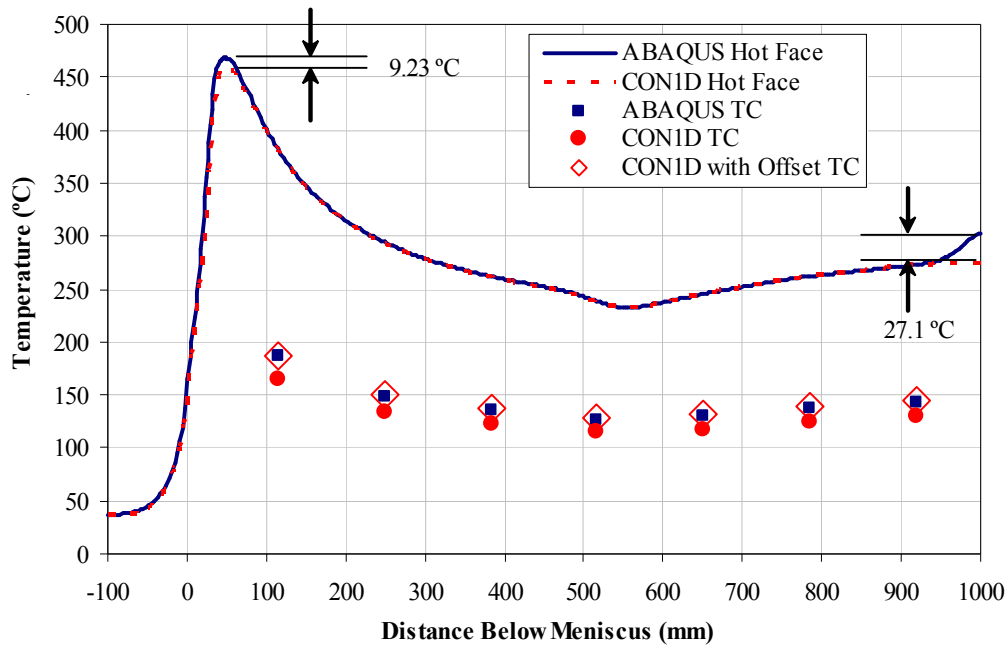


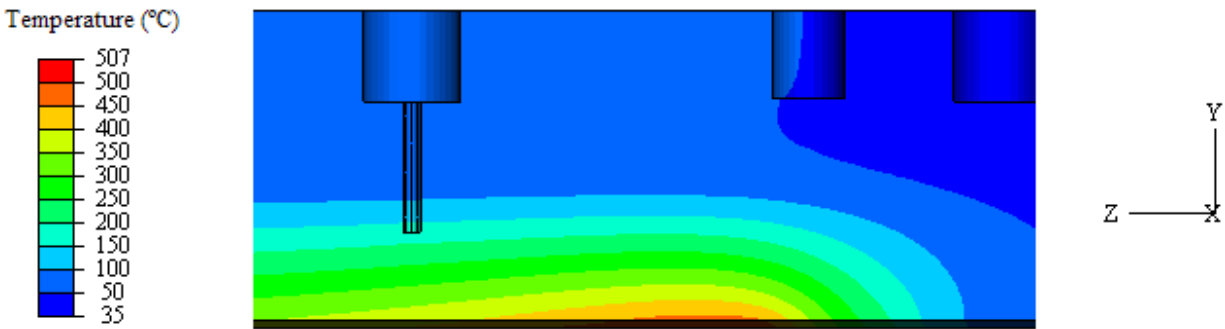
Figure 11. Full three-dimensional model temperature results (°C)

Figure 12 shows the 3-D hot face temperatures extracted along the plane of symmetry compared with the hot face temperatures from CON1D. The two programs match very well (typically within 2 °C) except around the areas with strong three-dimensional effects. Maximum errors are 9.2 °C near the heat flux peak and 27 °C at mould bottom, where the water slots end.



**Figure 12. Hot face and thermocouple temperatures comparison between CON1D and Abaqus**

Figure 13 shows the temperature contours around the area of peak heat flux, highlighting the localized thermal effects at this location. Although the CON1D model is least accurate at the hot face at this location, its two-dimensional mould temperature calculation in the vertical slice allows it to achieve acceptable accuracy.



**Figure 13. Temperature contours around the peak heat flux**

The temperatures predicted at all seven of the thermocouple locations in the mould compare closely with the offset CON1D values in Figure 12. The topmost of the eight bolt holes does not have a thermocouple and the middle hole in Figure 13 is for alignment. The results are tabulated in Table I and illustrated in Figure 12. The temperatures match almost exactly (within 1.4 °C or less), which is within the finite-element discretization error. This is a great improvement over the error of 12 to 21 °C produced by CON1D without the offset. Even when the heat flux peak was lowered 80mm to the level of the first thermocouple to produce maximum 3-D effects, the error in the CON1D prediction for that thermocouple was only -3.4 °C. Figure 12 also shows that the CON1D offset method is independent of heat flux, since the same offset was applied to all thermocouples. This means that a given mould geometry needs to be modelled in 3-D only once prior to conducting parametric studies using CON1D. In addition to its increased speed and ease-of-use, the CON1D model includes powerful additional calculations of the interfacial gap and solidifying shell. Thus, calibrating the CON1D model using the offset method to incorporate the 3-D ABAQUS results, unleashes a powerful and accurate tool to study continuous casting phenomena.

**Table I. Narrow-face Thermocouple Temperature Comparison**

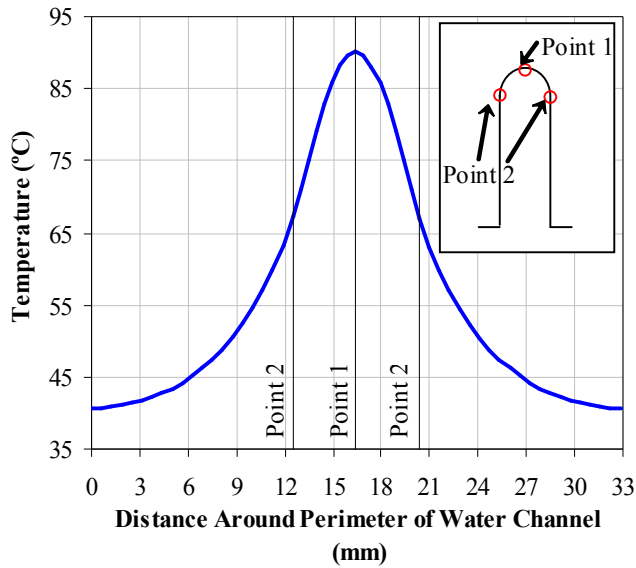
Distance Below Meniscus	3-D model	CON1D		CON1D with Offset	
	Temperature	Temperature	Difference	Temperature	Difference
mm	°C	°C	°C	°C	°C
115	186.6	165.4	-21.2	187.5	0.9
249	148.9	133.6	-15.3	150.0	1.1
383	135.7	122.5	-13.2	136.7	1.0
517	126.3	114.7	-11.6	127.4	1.1
651	129.8	118.0	-11.8	131.1	1.3
785	137.6	124.9	-12.7	139.0	1.4
919	142.9	129.6	-13.2	144.3	1.4

**Wide Face**

In Table II, ABAQUS and CON1D output results are compared along the direction of the mould perimeter at the calibration distance, 219 mm below the meniscus. The temperature at the cold face is tabulated at two points. As expected, point 1 is always hotter (around 90 °C) than point 2 (around 76 °C). The CON1D predicts temperature of the water slot root (cold face) to be 81.4°C, which lies in between these two values. Water slot temperatures near the bolt hole are hotter than those near the symmetry plane. Figure 14 shows the temperature profile around the perimeter of a wide face water channel.

**Table II. Wide face ABAQUS and CON1D comparison**

Parameter	3-D	CON1D
Hot face temperatures	237.2 - 243 °C	237.4 °C
Cold face temperatures in the cooling channels: Point 1- closest point of curved channel root to the hot face Point 2- first straight points after the curve	Point 1- 89.44 – 91.43 °C Point 2- 75.08 – 77.75 °C	81.4 °C
Temperature at the thermocouple location	143.9°C	143.90 °C (with offset)

**Figure 14. Temperature profile around perimeter of wide face water channel****Table III. Simulation Conditions**

Carbon Content, $C\%$	0.045	%
Liquidus Temperature, $T_{liq}$	1531	°C
Solidus Temperature, $T_{sol}$	1509	°C
Steel Density, $\rho_{steel}$	7400	kg/m <sup>3</sup>
Steel Emissivity, $\epsilon_{steel}$	0.8	-
Initial Cooling Water Temperature, $T_{water}$	33	°C
Cooling Water Velocity, $V_{water}$	8.5	m/s
Mould Emissivity, $\epsilon_{mould}$	0.5	-
Mould Slag Solidification Temp., $T_{fsol}$	1183	°C
Mould Slag Conductivity, $k_{solid}, k_{liquid}$	1.0, 1.5	W/mK
Air Conductivity, $k_{air}$	0.06	W/mK
Slag Layer/Mould Resistance, $r_{contact}$	9.5E-5	m <sup>2</sup> K/W
Mould Powder Viscosity at 1300°C, $\mu_{1300}$	0.9	Poise
Viscosity Temp.-dependence exponent, $n$	2.7	-
Slag Density, $\rho_{slag}$	2600	kg/m <sup>3</sup>
Slag Absorption Factor, $a$	250	m <sup>-1</sup>
Slag Refractive Index, $m$	1.667	-
Slag Emissivity, $\epsilon_{slag}$	0.9	-
Mould Powder Consumption Rate, $Q_{slag}$	0.0714	kg/m <sup>2</sup>
Pour Temperature, $T_{pour}$	1545	°C
Slab Geometry, width $\times$ thickness $W \times N$	1420 $\times$ 70	mm $\times$ mm
Nozzle Submergence Depth, $d_{nozzle}$	150	mm
Oscillation Mark Geometry, $d_{mark} \times w_{mark}$	0.08 $\times$ 1.5	mm $\times$ mm
Mould Oscillation Frequency, $freq$	325	cpm
Oscillation Stroke, $stroke$	6.0	mm



## VALIDATION WITH PLANT DATA AND PARAMETER STUDY

After verifying that the CON1D model matches with the full 3-D model, the next important step is to validate CON1D results with plant data and to check the accuracy of the model under different casting conditions.

### Database Comparison

A large database of plant data was compared with CON1D simulation results. The database contains more than 700 average values of heat flux, thermocouple temperatures and mould powder consumption, recorded from the wide faces during stable casting periods where the most important casting parameters, including casting speed and slab width, were constant for a period of at least 30 minutes. These data were downloaded from the mould thermal monitoring (MTM) system of the level 2 control system.

The first comparison with plant data was done for the average mould heat flux (from the cooling water) for different casting speeds. The data were divided according to mould copper thickness into thick new plates (with 0 to 5 mm mould wear) and thin old plates (with 10 to 15 mm mould wear). The trend lines match with CON1D predictions, as shown in Figure 15. This match is partly due to the effect of thinner shell decreasing thermal resistance at higher casting speed and thinner mould lowering mould thickness, which both increase heat flux. The realistic input data, given in Table III allow CON1D to capture these effects. The match was improved by accounting for the changes in the solid slag layer velocity, as discussed in the next section of this paper. In addition to investigating mould temperatures, shell growth and interfacial phenomena, this calibrated and validated model enables extrapolation to predict behaviour at higher casting speeds.

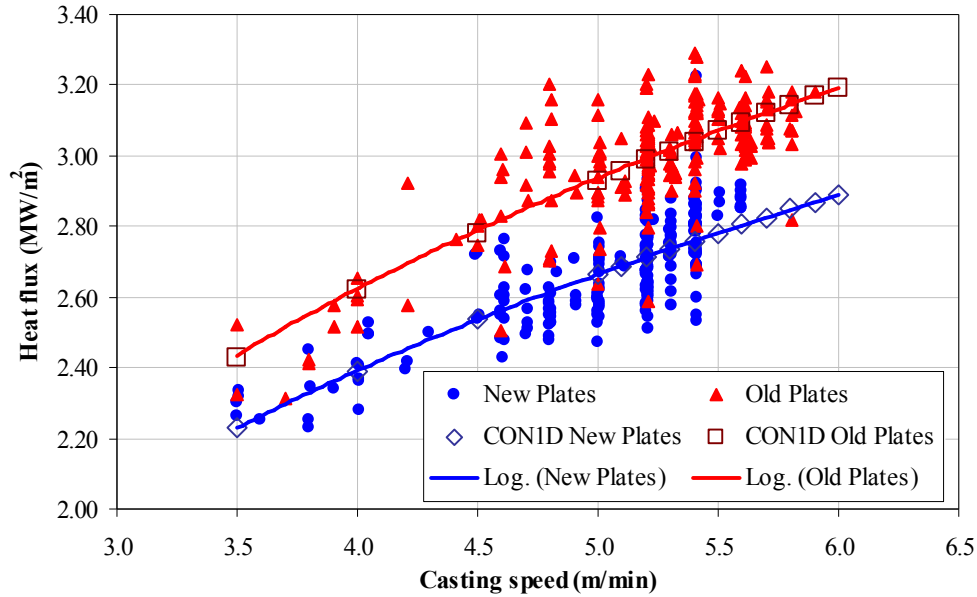


Figure 15. CON1D mean heat flux compared to plant data

### Velocity ratio between Solid Slag Layer and Steel Shell

The solid slag layer is assumed to move down the mould at a time-averaged velocity (and location: i.e. thickness of the liquid layer). This ratio ranges between zero (if the slag layer is attached to the mould) and the casting speed (if the slag layer is attached to the shell). This ratio between the solid slag speed and the casting speed must be input to the CON1D model. For a given powder consumption rate, this controls the average thickness of the slag layer, which greatly influences mould heat flux. A rough estimate of this ratio is given by:

$$\frac{V_{flux}}{V_C} = \frac{Q_{MP}}{\rho d_{slag}} \quad (2)$$

Where  $V_{flux}$  is the velocity of solid slag layer (m/min)  
 $V_C$  is the casting speed (m/min)  
 $Q_{MP}$  is the mould powder consumption (kg/m<sup>2</sup>)  
 $\rho$  is the mould slag density (kg/m<sup>3</sup>)  
 $d_{slag}$  is the slag layer thickness (m)

In practice, this velocity ratio varies with distance down the mould, which was characterized in this work to increase linearly between two values. At the meniscus, the ratio is zero, because the solid slag sticks to the mould wall and is relatively undisturbed due to the low friction associated with the liquid slag layer lubrication. At mould exit, Equation (2) is applied, based on the typical thickness of the solid slag layer that was measured at mould exit.

Slag films fragments previously taken from mould exit of the DSP caster ranged from 50 to 500 microns in thickness<sup>4</sup>. Because most of these fragments were split in the longitudinal direction, an average thickness of 200 microns was used in the first approximation of the velocity ratio. Further velocity ratios were found as a function of casting speed for both new and old mould plates, to match the average heat fluxes from the plant data. These two sets of ratios are plotted in Figure 16, and compared with mould powder consumption.

The velocity ratio has a strong correlation with the mould powder consumption, as given in Equation (2). This relation also can be seen in Figure 16, where the both velocity-ratio curves drop with increasing casting speed in the same way as the mould powder consumption. This finding is logical because a higher casting speed increases both hot face temperature and shell surface temperature in the mould. This encourages a hotter, thicker liquid slag layer, which extends further down the mould, which encourages the solid slag layer to remain more attached to the mould wall, producing a lower velocity. Furthermore, the higher hot face temperature tends to keep the mould slag above its glass transition temperature, making slag fracture less likely and thus lower average velocity ratio at higher casting speed.

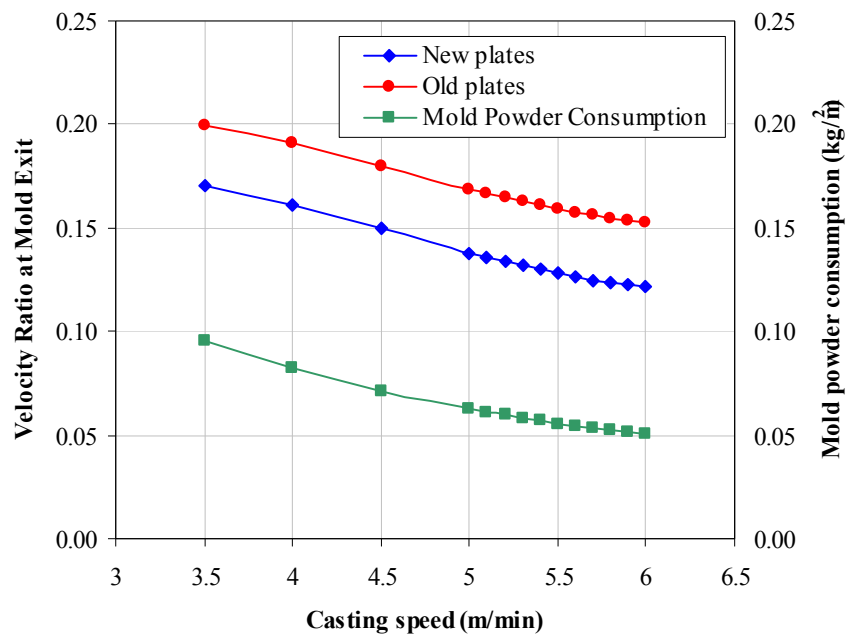


**Figure 16. Effect of casting speed on consumption and velocity ratios in new (thick) and old (thin) mould plates**

Mould heat flux varies with casting speed, velocity ratio and mould plate thickness. The CON1D results indicate that the velocity ratio itself varies with plate thickness. In new (thicker) plates, the mould hot face temperature is higher, which has a similar effect to increasing casting speed. Thus, the velocity ratio is expected to drop with new thin plates. The actual speed of the moving solid slag layer is not easily measured. Thus, the application of calibrated and validated models such as CON1D is important to achieve the understanding of mould phenomena necessary to extrapolate plant data to new conditions and to solve quality problems.

#### Temperature Validation

Plant data were obtained from a mould instrumented with forty thermocouples, as part of the standard MTM system to evaluate further the CON1D predictions. A period of 23 minutes of stable casting at a speed of 5.2 m/min and a width of 1328 mm was chosen for this comparison, due to its stability in the thermocouples measurements. The meniscus level was measured to be 100 mm below the top of the mould. The thermocouple numbers and positions are listed in Table IV and shown in Figure 17. Their 15mm depth below the hot face was offset by 2.41mm to 12.59 mm for CON1D.

**Table IV. Thermocouples used in the comparison with plant data**

Row	Thermocouple Number	Distance Below Meniscus (mm)
1st	2, 3, 4, 5, 6, 22, 23, 24, 25, 26	75
2nd	15, 35	200
3rd	16, 36	325
4th	9, 10, 11, 12, 13, 29, 30, 31, 32, 33	450

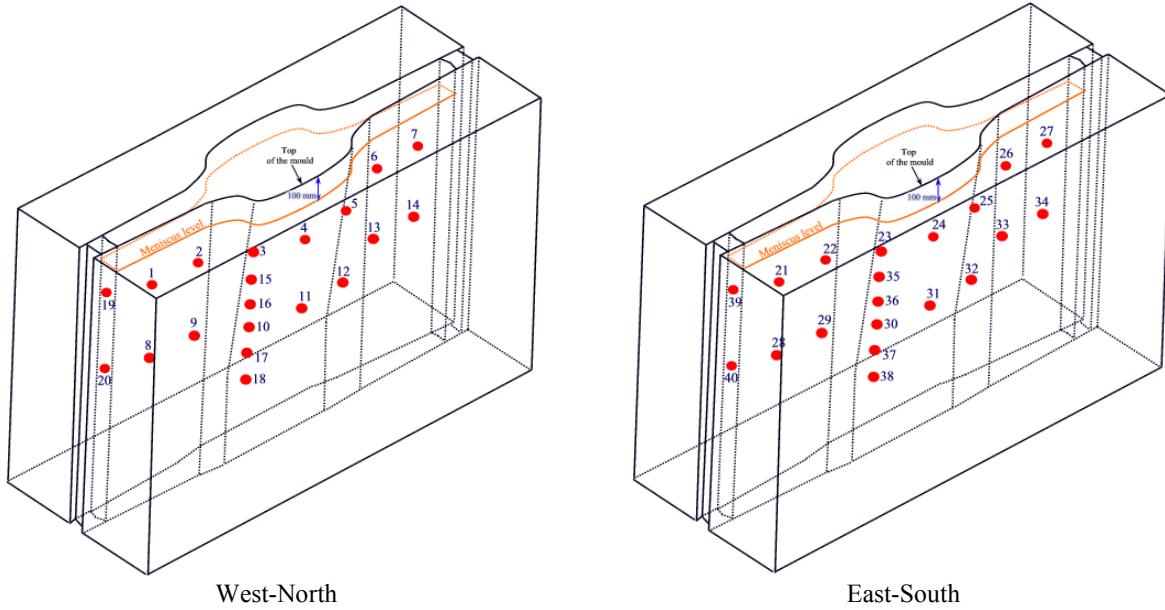


**Figure 17. Thermocouple numbers in the DSP mould**

The predicted hot face temperature profile, cold face (water slot root) temperature profile and thermocouple temperatures from CON1D are shown in Figure 18. This figure also shows the average of the measured temperatures, which are slightly lower. This might be due to minor contact problems causing the thermocouple temperatures to drop, or if boiling in the water channels caused the mould temperature to drop. Scale formation in the water channels would cause the mould temperature to be too high.

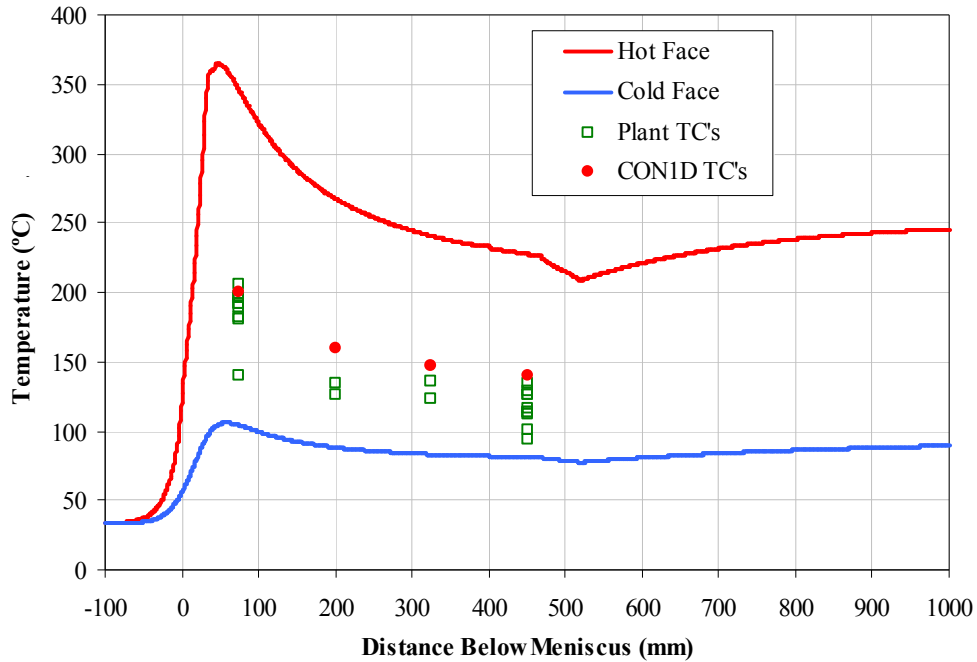


**Figure 18. Predicted thermocouple temperature compared with plant data in the considered period**

### Parametric Study

The verified, calibrated, and validated CON1D model is being applied to investigate a range of mould thermal phenomena, including high-speed casting, mould powder properties, scale formation in the water channels and breakout prediction. The effect of mould plate thickness on interfacial gap phenomena is investigated in the following section.

The effect of casting speed and mould plate thickness on various parameters at mould exit are shown in Figure 19 to Figure 22. Increasing casting speed naturally increases the mould hot face temperature and decreases the shell thickness. This causes the slab surface temperature to increase, although the increased heat flux with increasing casting speed tends to counter this trend. Slag layer thickness decreases with casting speed, owing to the smaller slag consumption rate, but the opposing effect of lower solid slag velocity ratio tends to lessen this trend.

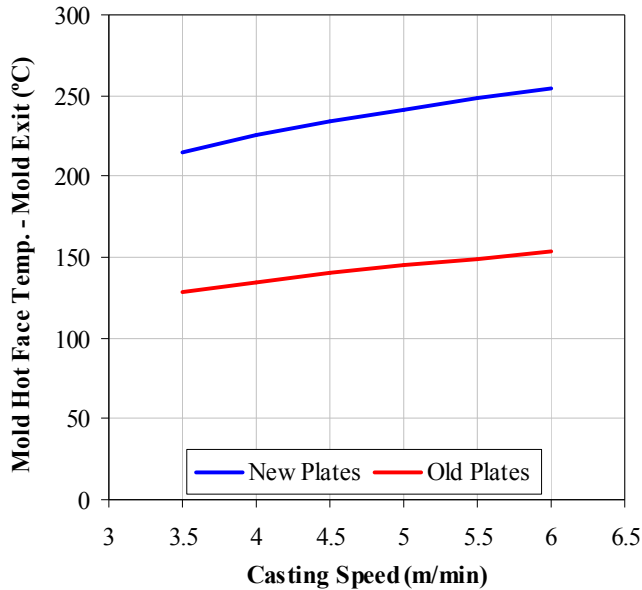


Figure 19. Effect of casting speed on mould hot face temp.

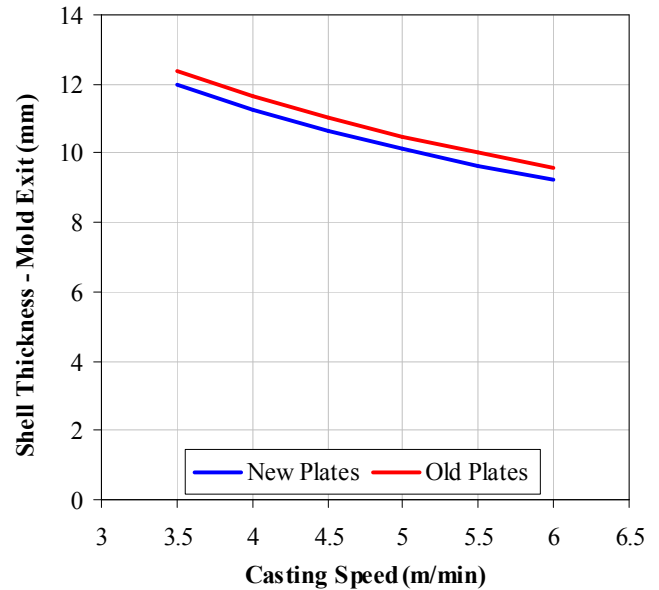


Figure 20. Effect of casting speed on shell thickness

Increasing the mould plate thickness (with new plates) naturally increases the hot face temperature. This lowers the solid slag layer velocity, (Figure 16), which produces a thicker slag layer, as shown in Figure 22. Together with the extra resistance of the thicker mould plate, this decreases the heat flux. This causes the shell thickness to decrease and slab surface temperature to increase.

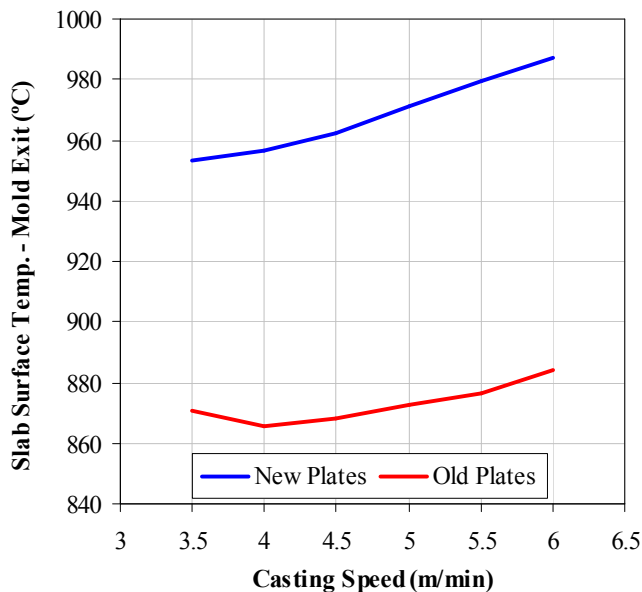


Figure 21. Effect of casting speed on slab surface temperature

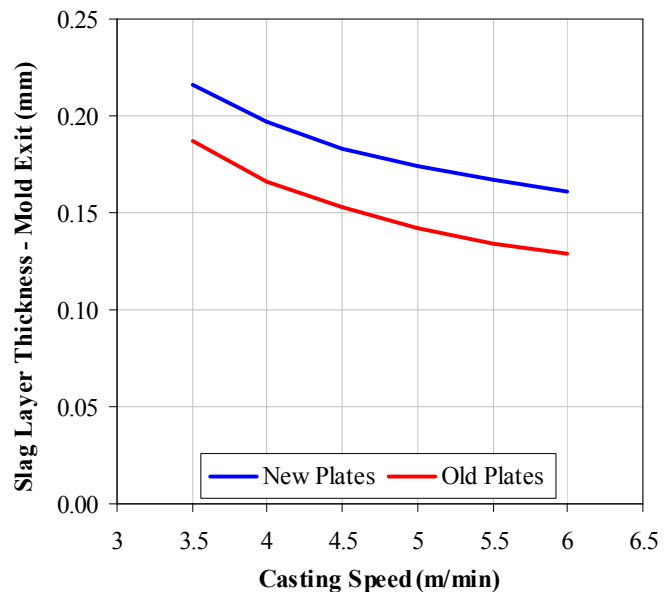


Figure 22. Effect of casting speed on slag layer thickness

## CONCLUSIONS

This work summarizes the development of an accurate computational tool for modelling heat transfer in the thin-slab continuous casting mould at the Corus DSP. Work towards this end includes model verification with a complete thermal 3-D analysis of the entire complex mould geometry, model calibration using the offset method to match thermocouple measurements and model validation with over 700 sets of plant data from an instrumented mould. The CON1D model is then applied together with plant measurements to gain a new insight into the effects of casting speed and mould plate thickness on mould heat transfer. Project findings include:

1. Increasing casting speed causes a thinner solidified steel shell, higher heat flux, higher mould hot face temperature, a thinner slag layer and lower solid slag layer velocity.
2. Increasing mould plate thickness increases hot face temperature, lowers solid slag layer velocity, increases slag layer thickness, and lowers mould heat flux.

The CON1D model is being applied to gain further insight into continuous casting of thin slabs, including the extrapolation of model predictions of heat transfer and interfacial phenomena to higher casting speed and the optimisation of mould taper, mould distortion, and funnel design.

## ACKNOWLEDGEMENTS

The authors wish to thank the member companies of the Continuous Casting Consortium and the National Science Foundation (Grant # 05-00453) for support of this work, the National Center for Supercomputing Applications for computational resources, and personnel at Corus DSP for plant data and support.

## REFERENCES

1. Meng, Y. and B.G. Thomas, "Heat Transfer and Solidification Model of Continuous Slab Casting: CON1D", *Metallurgical & Materials Transactions*, Vol. 34B, No. 5, Oct., 2003, pp. 685-705.
2. Langeneckert, Melody, "Influence of Mould Geometry on Heat Transfer, Thermocouple and Mould Temperatures in the Continuous Casting of Steel Slabs." M.S. Thesis, University of Illinois at Urbana-Champaign, 2001.
3. ABAQUS 6.6-1. 2006, ABAQUS, Inc., 166 Valley Street, Providence, RI 02909-2499.
4. J.A. Kromhout, S. Melzer, E.W. Zinngrebe, A.A. Kamperman and R. Boom, "Mould Powder Requirements for High-Speed Casting." *Proc. 2006 Int. Symposium on Thin Slab Casting and Rolling*, Guangzhou, 2006, The Chinese Society for Metals: 306-313.